

### Why Did Incorporation of Acrylonitrile to a Linear Polyethylene Become Possible? Comparison of Phosphine–Sulfonate Ligand with Diphosphine and Imine–Phenolate Ligands in the Pd-Catalyzed Ethylene/Acrylonitrile Copolymerization

Kyoko Nozaki,<sup>\*,†</sup> Shuhei Kusumoto,<sup>†</sup> Shusuke Noda,<sup>†</sup> Takuya Kochi,<sup>†,§</sup>  
Lung Wa Chung,<sup>‡</sup> and Keiji Morokuma<sup>\*,‡</sup>

*Department of Chemistry and Biotechnology, Graduate School of Engineering, The University of Tokyo, 7-3-1 Hongo, Bunkyo-Ku, Tokyo 113-8656, Japan, and Fukui Institute for Fundamental Chemistry, Kyoto University, Takano-Nishishiraki-cho, 34-4, Sakyo-ku, Kyoto 606-8103, Japan*

Received June 3, 2010; E-mail: nozaki@chembio.t.u-tokyo.ac.jp

**Abstract:** Palladium-catalyzed coordination–insertion copolymerization of ethylene with acrylonitrile (AN) proceeded only by using phosphine–sulfonate (P–SO<sub>3</sub>) as a ligand among the neutral and anionic ligands we examined, those are phosphine–sulfonate (P–SO<sub>3</sub>), diphosphine (P–P), and imine–phenolate (N–O). In order to answer a question that is unique for P–SO<sub>3</sub>, theoretical and experimental studies were carried out for the three catalyst systems. By comparing P–SO<sub>3</sub> and P–P, it was elucidated that (i) the  $\pi$ -acrylonitrile complex [(L–L')PdPr( $\pi$ -AN)] is less stable than the corresponding  $\sigma$ -complex [(L–L')PdPr( $\sigma$ -AN)] in both the phosphine–sulfonate complex (L–L' = P–SO<sub>3</sub>) and the diphosphine complex (L–L' = P–P) and (ii) the energetic difference between the  $\pi$ -complex and the  $\sigma$ -complex is smaller in the P–SO<sub>3</sub> complexes than in the P–P complexes. Thus, the energies of the transition states for both AN insertion and its subsequent ethylene insertion relative to the most stable species [(L–L')PdPr( $\sigma$ -AN)] are lower for P–SO<sub>3</sub> than for P–P. The results nicely explain the difference between these two types of ligands. That is, ethylene insertion subsequent to AN insertion was detected for P–SO<sub>3</sub>, while aggregate formation was reported for cationic [(L–L')Pd(ChCNCH<sub>2</sub>CH<sub>3</sub>)] complex. Aggregate formation with the cationic complex can be considered as a result of the retarded ethylene insertion to [(L–L')Pd(ChCNCH<sub>2</sub>CH<sub>3</sub>)]. In contrast, theoretical comparison between P–SO<sub>3</sub> and N–O did not show a significant energetic difference in both AN insertion and its subsequent ethylene insertion, implying that ethylene/AN copolymerization might be possible. However, our experiment using [(N–O)PdMe(lutidine)] complex revealed that  $\beta$ -hydride elimination terminated the ethylene oligomerization and, more importantly, that the resulting Pd–H species lead to formation of free N–OH and Pd(0) particles. The  $\beta$ -hydride elimination process was further studied theoretically to clarify the difference between the two anionic ligands, P–SO<sub>3</sub> and N–O.

#### Introduction

Functionalized linear polyethylene finds wide application due to its toughness accompanied by adhesion ability. Coordination copolymerization of ethylene with polar comonomers has attracted much attention as one of the most promising synthetic methods toward the syntheses of functionalized polyethylenes in the past decade.<sup>1–3</sup> Among the polar monomers, acrylonitrile (AN) was one of the most challenging monomers to incorporate

for years and intensive efforts were devoted using experimental<sup>4,5</sup> and theoretical<sup>6–11</sup> approaches.

In 2001, it was predicted that the energy barrier for 2,1-insertion of AN into an alkyl–palladium bond is energetically accessible when it starts from a  $\pi$ -AN complex of cationic diimine/Pd species.<sup>12</sup> One year later, it was theoretically

<sup>†</sup> The University of Tokyo.

<sup>‡</sup> Kyoto University.

<sup>§</sup> Present address: Department of Chemistry, Faculty of Technology, Keio University, 3-14-1 Hiyoshi, Kohoku-ku, Yokohama, Kanagawa 223-8522, Japan.

(1) Ittel, S. D.; Johnson, L. K.; Brookhart, M. *Chem. Rev.* **2000**, *100*, 1169–1203.

(2) Berkefeld, A.; Mecking, S. *Angew. Chem., Int. Ed.* **2008**, *47*, 2538–2542.

(3) Nakamura, A.; Ito, S.; Nozaki, K. *Chem. Rev.* **2009**, *109*, 5215.

(4) Groux, L. F.; Weiss, T.; Reddy, D. N.; Chase, P. A.; Piers, W. E.; Ziegler, T.; Parvez, M.; Benet-Buchholz, J. *J. Am. Chem. Soc.* **2005**, *127*, 1854–1869.

(5) Wu, F.; Foley, S. R.; Burns, C. T.; Jordan, R. F. *J. Am. Chem. Soc.* **2005**, *127*, 1841–1853.

(6) Deubel, D. V.; Ziegler, T. *Organometallics* **2002**, *21*, 4432–4441.

(7) Deubel, D. V.; Ziegler, T. *Organometallics* **2002**, *21*, 1603–1611.

(8) Szabo, M. J.; Galea, N. M.; Michalak, A.; Yang, S. Y.; Groux, L. F.; Piers, W. E.; Ziegler, T. *Organometallics* **2005**, *24*, 2147–2156.

(9) Szabo, M. J.; Galea, N. M.; Michalak, A.; Yang, S. Y.; Groux, L. F.; Piers, W. E.; Ziegler, T. *J. Am. Chem. Soc.* **2005**, *127*, 14692–14703.

(10) Yang, S. Y.; Szabo, M. J.; Michalak, A.; Weiss, T.; Piers, W. E.; Jordan, R. F.; Ziegler, T. *Organometallics* **2005**, *24*, 1242–1251.

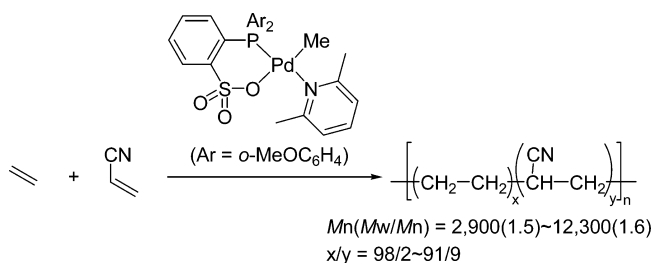
(11) Szabo, M. J.; Jordan, R. F.; Michalak, A.; Piers, W. E.; Weiss, T.; Yang, S. Y.; Ziegler, T. *Organometallics* **2004**, *23*, 5565–5572.

suggested that, for the cationic diimine/Pd complex, formation of an extremely stable  $\sigma$ -AN complex reduces the population of the  $\pi$ -AN complex so significantly that the following AN insertion becomes impossible.<sup>13</sup> On the basis of these theoretical studies, the use of neutral or anionic metal complexes was suggested to facilitate insertion by destabilizing the  $\sigma$ -AN complex with respect to the  $\pi$ -AN complex. For example, Deubel and Ziegler predicted the Grubbs-type imine–phenolato complex (neutral complex) to be superior to the Brookhart-type diimine complex (cationic complex) because the  $\pi$ -AN complex is more stabilized than the  $\sigma$ -AN complex in the Grubbs system.<sup>6,7</sup> They further found a unique olefin insertion pathway for the unsymmetrical bidentate ligand system. That is, among the cis/trans isomers of complexes  $[(L-L')Ni(C_2H_5)(\pi\text{-AN})]$ , the more stable isomer, in which the ethyl group is trans to the oxygen atom, first isomerizes to the less stable isomer, in which the ethyl group is trans to the nitrogen atom. Subsequently, AN insertion takes place via the lower energy TS than the one from the other isomer, resulting in the more stable  $\alpha$ -cyanoalkyl complex, in which the alkyl group is trans to the oxygen atom. Further design of neutral and anionic complexes was reported by Piers and Ziegler.<sup>6,8–11</sup>

Eventually in 2005, 2,1-insertion of AN into a methyl–palladium bond was observed experimentally for cationic<sup>5,14,15</sup> and neutral or anionic palladium species.<sup>4,15</sup> Jordan employed cationic complexes bearing neutral bidentate ligands such as bisimidazole, bipyridine, and diimine for observation of the AN insertion, while Piers used neutral and even anionic complexes with negatively charged imine–phenolate and diazene–phenolato ligands. In both cases, formation of insoluble oligomeric assemblies of  $\alpha$ -cyanoalkylpalladium species was suggested to hamper the coordination polymerization of AN.<sup>9–11</sup> Concurrently, aggregate formation was proven to be reversible by trapping the monomeric unit with strong donor ligands, such as phosphines. Consequently, subsequent olefin insertion should be possible if the insertion TS is reasonably low relative to the most stable complex (resting state).

In order to obtain a copolymer of ethylene with polar monomers, it is indispensable that ethylene insertion takes place subsequent to insertion of a polar monomer. Nevertheless, studies on subsequent ethylene insertion are rather limited. Insertion copolymerization of ethylene with methyl acrylate (MA) was studied both theoretically and experimentally for the diimine/Pd system, but ethylene insertion was an event after chain walking of Pd proceeded to form a stable six-membered chelate.<sup>16–19</sup> Goddard studied ethylene insertion subsequent to insertion of vinyl acetate (VAc) or vinyl chloride (VC) but did not discuss the reaction after AN insertion.<sup>13</sup> The attempted copolymerization of ethylene with VAc was further studied by

Scheme 1



Brookhart.<sup>20</sup> Ziegler and Jordan also carried out DFT calculations on copolymerization of ethylene with polar monomers including AN and predicted that the activation energy for ethylene insertion subsequent to AN insertion is 27.1 kcal/mol with a neutral palladium complex.<sup>11</sup>

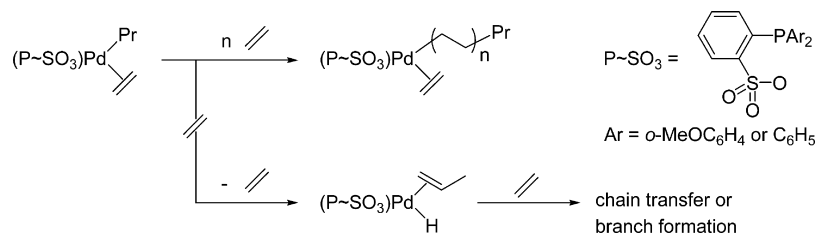
In 2007, we reported the first coordination–insertion copolymerization of ethylene with AN using an isolated palladium complex of a phosphine–sulfonate ligand as a catalyst (Scheme 1).<sup>21–31</sup> The product was a linear copolymer containing nitrile groups not only at the chain ends but also in the middle of the chain. Prompted by a question of why the polymer possessed a linear structure but not a branched one, we carried out theoretical studies on ethylene homopolymerization catalyzed by the phosphine–sulfonate Pd complex.<sup>32</sup> It was suggested that in the presence of an excess amount of ethylene, ethylene insertion predominates over  $\beta$ -hydride elimination and subsequent branch formation or chain-transfer reactions because the energy barriers for ethylene insertion and  $\beta$ -H elimination reactions were comparable (Scheme 2). At this stage, the remaining question to be resolved is why AN incorporation to the polyethylene chain became possible using the phosphine–sulfonate Pd complex.

In this paper first we report our attempts to perform ethylene/AN copolymerization using three different catalyst systems A–C, described in Figure 1 (section 1). It was revealed that the copolymer can be obtained only with the phosphine–sulfonate (P–SO<sub>3</sub>)/Pd complex A but not with diphosphine (P–P)/Pd complex B or imine–phenolato (N–O)/Pd complex C. Next, we report our theoretical studies on the three key steps of polymerization as described in Scheme 3 (section 2); (i)

- (12) von Schenck, H.; Stromberg, S.; Zetterberg, K.; Ludwig, M.; Akermarck, B.; Svensson, M. *Organometallics* **2001**, *20*, 2813–2819.
- (13) Philipp, D. M.; Muller, R. P.; Goddard, W. A.; Storer, J.; McAdon, M.; Mullins, M. *J. Am. Chem. Soc.* **2002**, *124*, 10198–10210.
- (14) Stojcevic, G.; Prokopchuk, E. M.; Baird, M. C. *J. Organomet. Chem.* **2005**, *690*, 4349–4355.
- (15) Wu, F.; Jordan, R. F. *Organometallics* **2006**, *25*, 5631–5637.
- (16) Johnson, L. K.; Mecking, S.; Brookhart, M. *J. Am. Chem. Soc.* **1996**, *118*, 267–268.
- (17) Mecking, S.; Johnson, L. K.; Wang, L.; Brookhart, M. *J. Am. Chem. Soc.* **1998**, *120*, 888–899.
- (18) Michalak, A.; Ziegler, T. *J. Am. Chem. Soc.* **2001**, *123*, 12266–12278.
- (19) Michalak, A.; Ziegler, T. *Organometallics* **2003**, *22*, 2660–2669.

- (20) Williams, B. S.; Leatherman, M. D.; White, P. S.; Brookhart, M. *J. Am. Chem. Soc.* **2005**, *127*, 5132–5146.
- (21) Kochi, T.; Noda, S.; Yoshimura, K.; Nozaki, K. *J. Am. Chem. Soc.* **2007**, *129*, 8948.
- (22) For the main-chain incorporation of other polar monomers using Pd/phosphine–sulfonate, see refs 24 and 26–30.
- (23) Drent, E.; van Dijk, R.; van Ginkel, R.; van Oort, B.; Pugh, R. I. *Chem. Commun.* **2002**, 744–745.
- (24) Kochi, T.; Yoshimura, K.; Nozaki, K. *Dalton Trans.* **2006**, 25–27.
- (25) Skupov, K. M.; Marella, P. R.; Simard, M.; Yap, G. P. A.; Allen, N.; Conner, D.; Goodall, B. L.; Claverie, J. P. *Macromol. Rapid Commun.* **2007**, *28*, 2033–2038.
- (26) Luo, S.; Vela, J.; Lief, G. R.; Jordan, R. F. *J. Am. Chem. Soc.* **2007**, *129*, 8946+.
- (27) Weng, W.; Shen, Z.; Jordan, R. F. *J. Am. Chem. Soc.* **2007**, *129*, 15450+.
- (28) Skupov, K. M.; Piche, L.; Claverie, J. P. *Macromolecules* **2008**, *41*, 2309–2310.
- (29) Borkar, S.; Newsham, D. K.; Sen, A. *Organometallics* **2008**, *27*, 3331–3334.
- (30) Guironnet, D.; Roesle, P.; Runzi, T.; Gottker-Schnetmann, I.; Mecking, S. *J. Am. Chem. Soc.* **2009**, *131*, 422–423.
- (31) Guironnet, D.; Caporaso, L.; Neuwald, B.; Gottker-Schnetmann, I.; Cavallo, L.; Mecking, S. *J. Am. Chem. Soc.* **2009**, *132*, 4418–4426.
- (32) Noda, S.; Nakamura, A.; Kochi, T.; Chung, L. W.; Morokuma, K.; Nozaki, K. *J. Am. Chem. Soc.* **2009**, *131*, 14088–14100.

Scheme 2



equilibrium between the  $\sigma$ -AN complexes **1** and the olefin  $\pi$ -complexes **2** or **4** (section 2.1), (ii) AN insertion **1**  $\rightarrow$  **2**  $\rightarrow$  **3**  $\rightarrow$  **6** in comparison to ethylene insertion **1**  $\rightarrow$  **4**  $\rightarrow$  **5** (section 2.2), and (ii) subsequent ethylene insertion **6**  $\rightarrow$  **7**  $\rightarrow$  **8**  $\rightarrow$  **9** in comparison to the subsequent AN insertion **6**  $\rightarrow$  **10**  $\rightarrow$  **11**  $\rightarrow$  **12** (section 2.3). For each of the three key steps, comparison between the two ligands, an anionic P–SO<sub>3</sub> and a neutral ligand P–P will be first discussed. Second, the data will be also compared to those with N–O and diimine (N–N) complexes.<sup>6,7,9</sup> Because no clear difference was found between P–SO<sub>3</sub> and N–O at this stage, we further continued the following studies. In section 3, it will be proven experimentally that, with the N–O/Pd system, polymerization was terminated by  $\beta$ -hydride elimination from alkylPd(N–O) to give PdH(N–O). This process leads to deactivation of catalyst by the following reductive elimination of free phenol (N–OH) from PdH(N–O). Finally, in section 4, the competing  $\beta$ -hydride eliminations from propylPd **1**  $\rightarrow$  **13**  $\rightarrow$  **14** and from  $\alpha$ -cyanopropylPd **15**

(analogous to **6**)  $\rightarrow$  **16**  $\rightarrow$  **17** will be discussed by comparing P–SO<sub>3</sub> and N–O ligands.

## Results and Discussion

**1. Attempted Copolymerization of Ethylene with AN in the Presence of Complexes A–C.** As reported in our previous communication, the copolymer possessing nitrile groups in the middle of the chain was obtained by copolymerization of ethylene with AN using complex **A**.<sup>21</sup> In contrast, the use of cationic complex **B** or neutral complex **C** under the same reaction conditions (3.0 MPa of ethylene, 0.5 mL of AN, and 0.01 mmol of the catalyst in 4.5 mL of toluene heated at 100 °C for 5 days) provided no polymeric materials after removal of all volatiles (see Supporting Information for experimental details). The different behavior of complex **A** from **B** and **C** was further studied in detail as follows.

**2. Theoretical Studies for Insertion of Ethylene and AN.** In our current theoretical studies, the same computational methods used in our previous study<sup>21</sup> (B3LYP<sup>33,34</sup>/6-31G\* and Lanl2dz<sup>35</sup>) was employed.<sup>36</sup> The energies ( $E+ZPC$ , with zero-point energy correction, before /) and free energies ( $G$ , after /) for all stationary points will be expressed relative to the  $\sigma$ -AN complex **1** in the following studies. In our experiment, we employed a lutidine complex **A** described in Scheme 1. The  $\sigma$ -AN complex [(P–SO<sub>3</sub>)PdPr( $\sigma$ -AN)] (**1a** in Scheme 4) is less stable than the pyridine complex [(P–SO<sub>3</sub>)PdPr(pyridine)], an analog of lutidine complex, but their energy difference of 4.3 kcal/mol<sup>37</sup> is conquerable under the reaction condition of a high concentration of AN. First, the equilibrium between the  $\sigma$ -AN

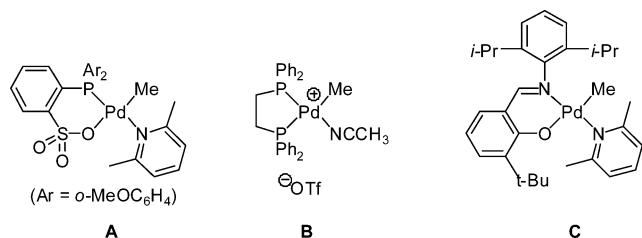
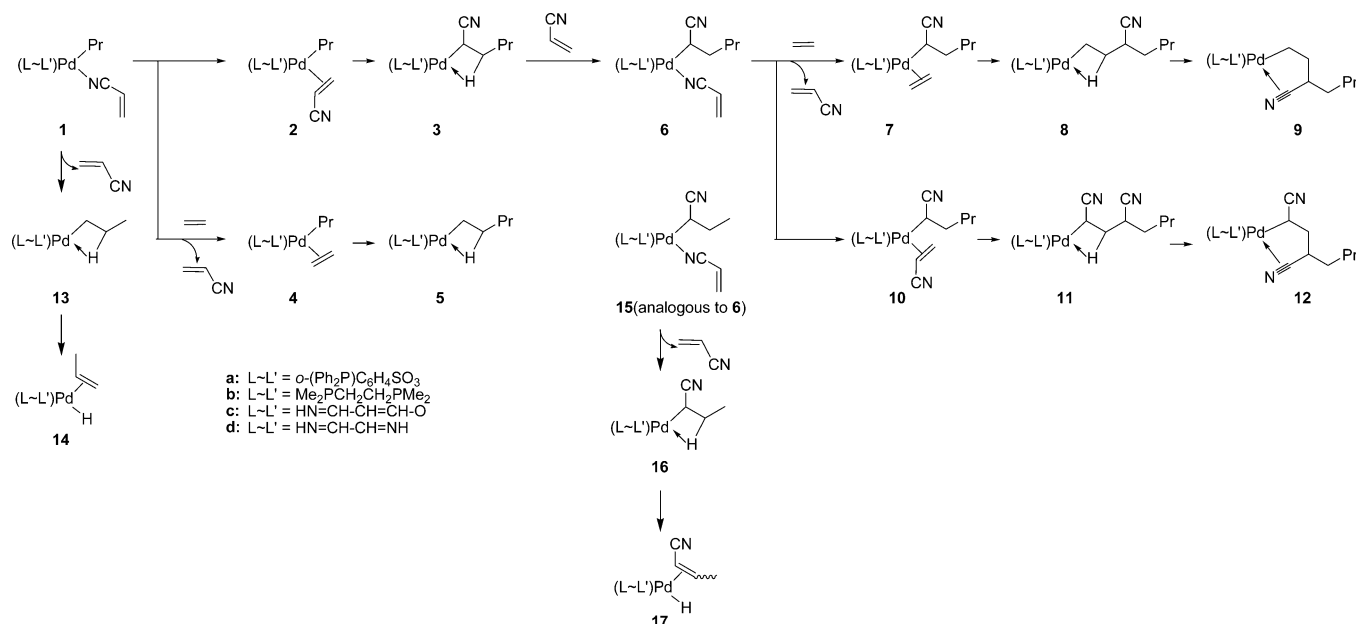
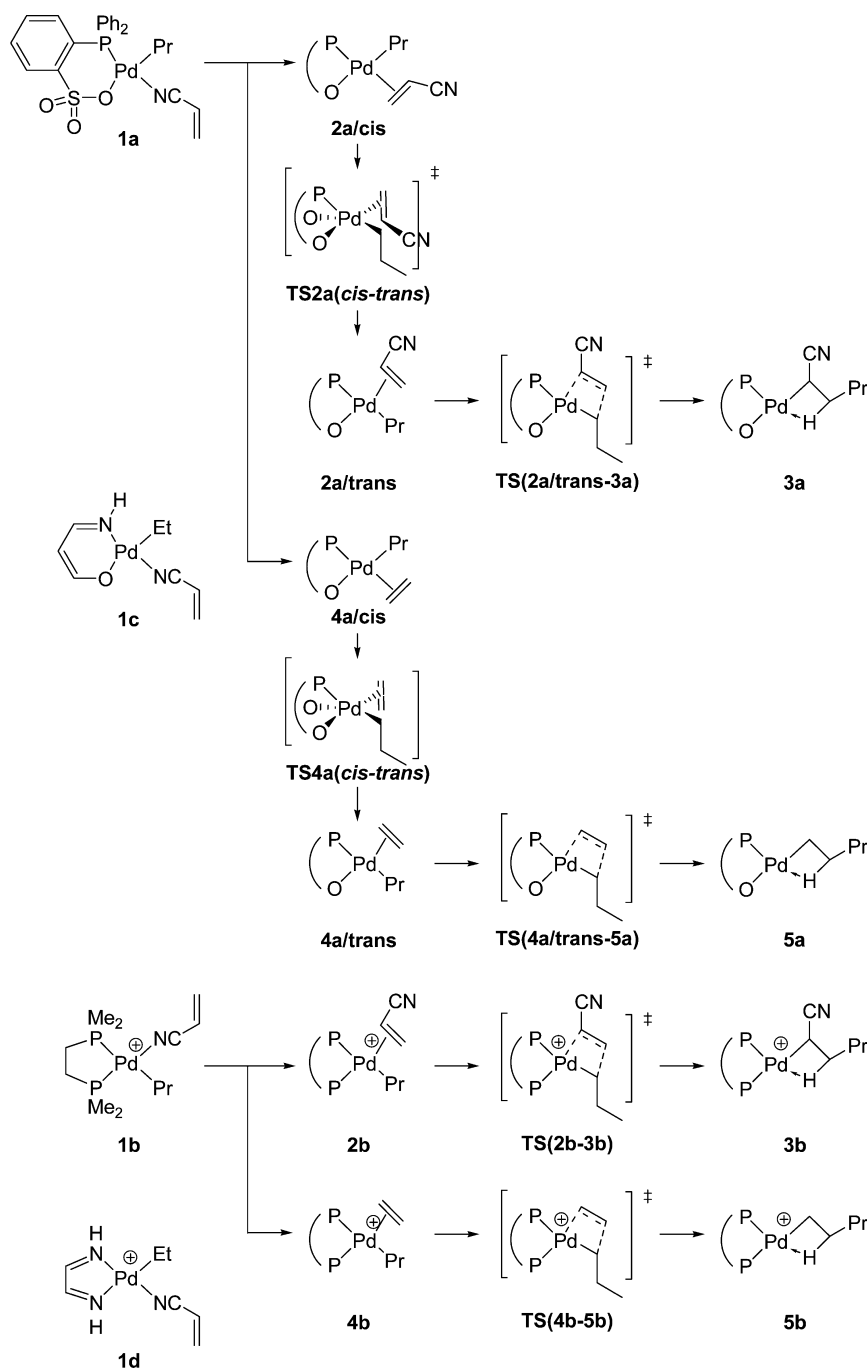


Figure 1. Examined catalysts for ethylene/AN copolymerization.

Scheme 3



Scheme 4



complex,  $[(L-L')PdPr(\sigma\text{-AN})]$  (1), and the  $\pi$ -AN complex,  $[(L-L')PdPr(\pi\text{-AN})]$  (2), was studied and the energies compared with that of the  $\pi$ -ethylene complex  $[(L-L')PdPr(\pi\text{-ethylene})]$  (4) (section 2.1; Scheme 4 and Figure 2). Second, AN insertion from the  $\pi$ -AN complex 2 was calculated and compared with our previous study on ethylene insertion (section 2.2; Scheme 4 and Figure 2). Third, subsequent ethylene or AN insertion to the  $\alpha$ -cyanoalkylPd species,  $[(L-L')Pd(ChCNCH_2Pr)(\sigma\text{-AN})]$  (6), was studied (section 2.3; Scheme 5 and Figure 3).

**2.1. Equilibrium between the  $\sigma$ -AN Complexes 1 with the Olefin  $\pi$  Complexes 2 or 4.** The energies of the  $\sigma$ - and  $\pi$ -AN complexes were calculated for the phosphine-sulfonato complexes 1a and 2a and are shown in Figure 2. It should be noted that there are cis/trans isomers due to the unsymmetrical nature of the phosphine-sulfonato ligand. The energies are described with reference to the more stable 1a, the cis isomer. Hereafter, the isomer having an X ligand (X = alkyl or H) and a neutral site of the bidentate ligand in cis positions to each other will

(33) Becke, A. D. *J. Chem. Phys.* **1993**, 98, 5648–5652.

(34) Lee, C. T.; Yang, W. T.; Parr, R. G. *Phys. Rev. B* **1988**, 37, 785–789.

(35) Hay, P. J.; Wadt, W. R. *J. Chem. Phys.* **1985**, 82, 270–283.

(36) Frisch, M. J. *Gaussian 03*, Revision C02; Gaussian, Inc.: Wallingford, CT, 2007.

(37) This number may be overestimated as the bulky lutidine experimentally used may have a weaker binding affinity than pyridine. The energy difference between lutidine complex and AN complex is estimated to be about 4.5 kcal/mol experimentally by the reaction of complex A with AN (see Supporting Information for experimental details).



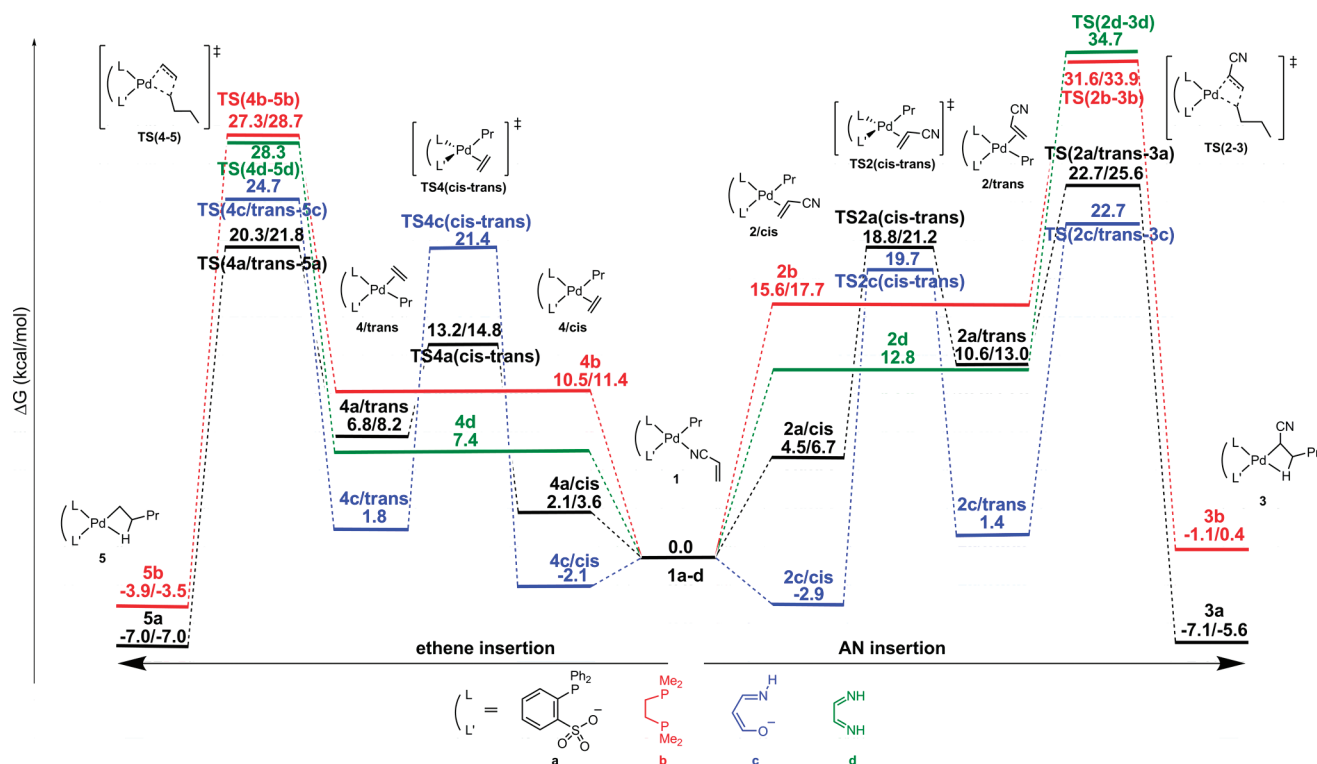


**Figure 2.** Energy profiles for the insertions starting from the  $\sigma$ -AN complexes **1a–d**. For complexes **1a** and **1b**, energies (E+ZPC, with zero-point energy correction, before /) and free energies (G, after /) are given in kcal/mol, relative to **1a** and **1b**, respectively. For complexes **1c** and **1d**, the data were taken from refs 6 and 7 and the free energy (G) values are expressed relative to **1c** or **1d**. For complexes **1c** and **1d**, only TSs were reported but not the products.

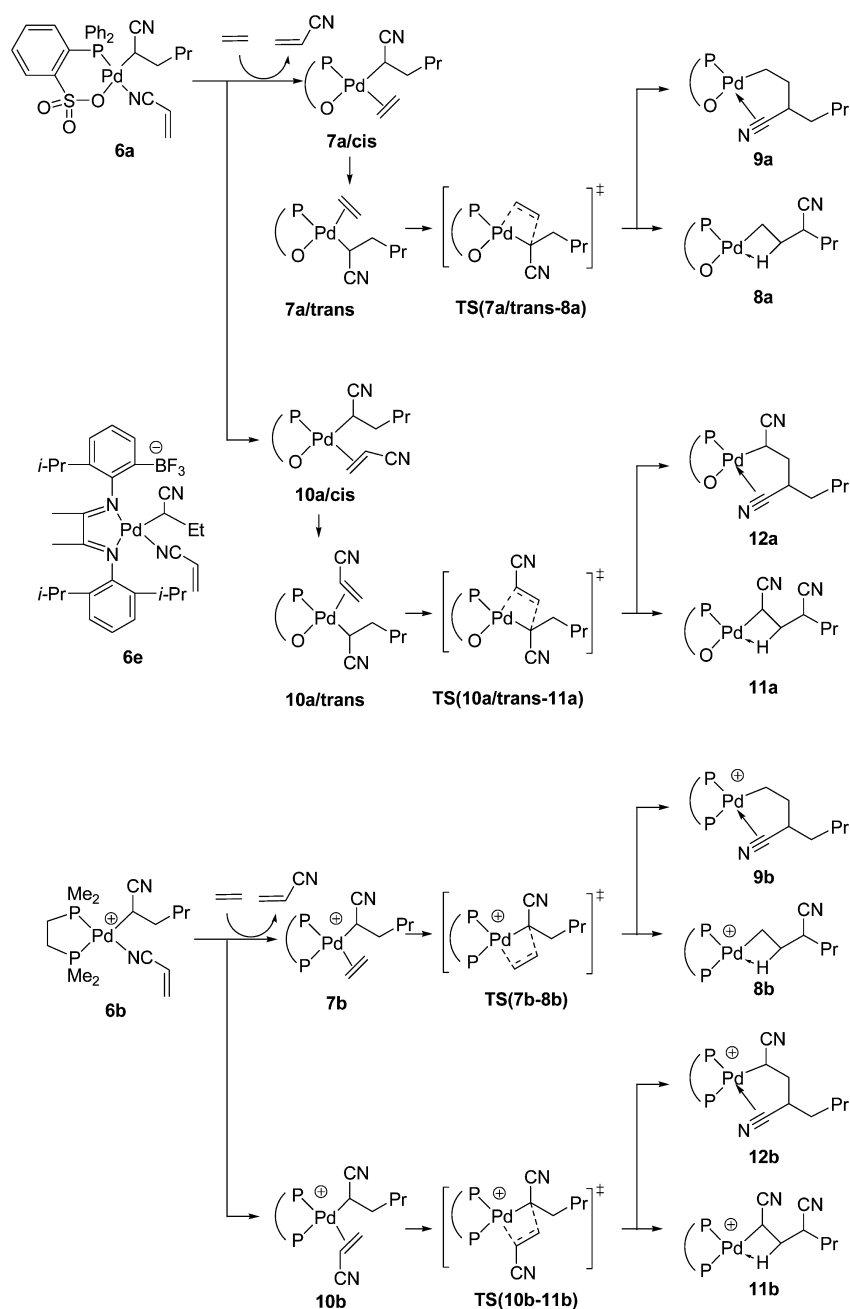
be described as cis for the united definition throughout the manuscript. In other words, an anionic site of the bidentate ligand and an L ligand (L = olefin or agostic C–H bond) are cis to each other in the cis isomer. For the cis/trans isomerization between **2a/cis** and **2a/trans**, pentacoordinate transition structure **TS2a(cis–trans)** was located, which is similar to our previous study for isomerization of [(P–SO<sub>3</sub>)PdPr(ethylene)].<sup>32</sup> The cis  $\pi$ -AN complex **2a/cis** is less stable than the  $\sigma$ -AN complex **1a** by 4.5/6.7 kcal/mol. The cis  $\pi$ -AN complex **2a/cis** can isomerize to the less stable isomer **2a/trans** with an energy of 10.6/13.0 kcal/mol via **TS2a(cis–trans)** with a barrier of 18.8/21.2 kcal/mol. Similarly, the energies were calculated for the  $\sigma$ - and  $\pi$ -AN diphosphine complexes **1b** and **2b**. The energy difference between the  $\pi$ -AN complexes **2** and the  $\sigma$ -AN complexes **1** was smaller for the P–SO<sub>3</sub> complexes (4.5/6.7 kcal/mol) than the P–P complexes (15.6/17.7 kcal/mol). For comparison, the stability of the  $\pi$ -AN complexes (**2c** and **2d**) relative to the  $\sigma$ -AN complexes (**1c** and **1d**) for the imine–phenolato (N–O) and diimine (N–N) complexes studied by Deubel and Ziegler<sup>6,7</sup> are also added to Figure 2. Among the four series of complexes **a–d**, the smallest energy difference between **1** and **2** was found for the N–O complexes, **1c** and **2c**.

The relative stability for  $\pi$ -ethylene complexes **4a–d** are also summarized in Figure 2. For the cationic complexes with neutral ligands, the  $\pi$ -ethylene complexes **4b** and **4d** are much more stable than the  $\pi$ -AN complexes **2b** and **2d**. In contrast, rather similar stability was observed for the neutral complexes with anionic ligands **4a**, **4c** and **2a**, **2c**. They can be explained by the fact that (i) the cationic complexes prefer the more electron-rich C=C bond of ethylene than the electron-deficient C=C bond of AN, where the  $\pi$ -complex formation is dominated by the  $\pi$ -electron donation from the olefin to the electron-deficient metal center, and (ii) back-donation from the more electron-

rich metal center to the  $\pi^*$ -orbital becomes more important and favorable in the neutral complexes. It is notable that for imine–phenolato Pd complexes **c**, the  $\pi$ -AN complex becomes even more stable than the  $\pi$ -ethylene complex, suggesting large stabilization from the back-donation.

**2.2. AN Insertion from the  $\pi$ -AN Complexes 2.** AN insertion from a  $\pi$ -AN complex was studied for both **2a** and **2b** and compared with the reported data for **2c** and **2d**. For reaction of AN with alkylpalladium species, the predominant 2,1-insertion was predicted theoretically<sup>11,12</sup> and proven experimentally.<sup>4,5</sup> Thus, the energies for all of the transition states for 2,1-insertion were calculated and are summarized in the Supporting Information. The favorable energetic profiles are sketched in Figure 2. For the 2,1-insertion of AN from cis and trans  $\pi$ -AN complexes **2a/cis** and **2a/trans**, we found the lowest energy TS for AN insertion is **TS(2a/trans–3a)**. Thus, for the P–SO<sub>3</sub> system, the more stable isomer **2a/cis** first isomerizes to the less stable isomer **2a/trans**, which then undergoes AN insertion via the lowest energy TS, **TS(2a/trans–3a)** with a barrier height of 22.7/25.6 kcal/mol relative to **1a**. This process, which is isomerization to the less stable  $\pi$ -complex followed by olefin insertion, corresponds to our previous study on ethylene insertion to propylPd species, that is, **4a/cis**  $\rightarrow$  **4a/trans**  $\rightarrow$  **5a**.<sup>32</sup> **TS(2a/trans–3a)** for AN insertion is higher in energy than **TS(4a/trans–5a)** for ethylene insertion by 2.4 kcal/mol, which nicely accords with our experimental results, which is the competing but preferential incorporation of ethylene over AN in the E/AN copolymer formation (Scheme 1). These results are also compared with the other ligand systems as follows. For the cationic complexes, AN insertion TSs **TS(2b–3b)** and **TS(2d–3d)** are much higher than ethylene insertion TSs **TS(4b–5b)** and **TS(4d–5d)**, respectively. In contrast, **1c** was calculated to kinetically favor AN insertion via **TS(2c/trans–3c)** over ethylene

Scheme 5



insertion via **TS(4c/trans-5c)** by 2.0 kcal/mol, which apparently suggested that E/AN copolymerization would be accomplishable with this neutral system (see sections 3 and 4 to see the real obstacles).<sup>38,39</sup>

**2.3. Subsequent Ethylene or AN Insertion to the  $\alpha$ -Cyanoalkyl Pd Species.** Since 2,1-insertion of AN to a methyl–palladium bond was experimentally found for cationic<sup>5,14,15</sup> and neutral

or anionic palladium species,<sup>4,15</sup> aggregate formation from the  $\alpha$ -cyanoalkyl complexes was suggested to be problematic for E/AN copolymerization.<sup>9,10</sup> Nevertheless, the aggregate should not be formed if subsequent ethylene insertion to the  $\alpha$ -cyanoalkyl complex is reasonably rapid. Even if the aggregate is formed, there must be a reversible pathway to eventually accomplish the subsequent ethylene insertion. The key energy values relative to **6a** and **6b**, the most stable isomers of  $[(L-L')Pd(ChCNCH_2Pr)(\sigma-AN)]$ , are summarized in Figure 3. The energies of **6a** and **6b** relative to **1a** and **1b** are  $-26.3/-12.9$  and  $-23.9/-11.2$  kcal/mol, respectively. As shown in Figure 3, the ethylene insertion via **6a**  $\rightarrow$  **7a/trans**  $\rightarrow$  **TS(7a/trans-8a)**  $\rightarrow$  **8a** requires a barrier of 27.5/27.8 kcal/mol relative to **6a**, 1.2/14.8 kcal/mol higher than that starting from **1a**. The TS seems to be conquerable under standard reaction conditions. After ethylene insertion, the  $\beta$ -agostic three-coordinate product

(38) Ziegler performed these calculations by a different functional (BP86). We calculated the key intermediates and transition states (**1c** and **TS(2c/trans-3c)**) by B3LYP functional to see the effect of the functionals on the reaction barrier. The energy level of **TS(2c/trans-3c)** relative to **1c** was calculated to be 21.8/24.7 kcal/mol by the B3LYP method, which is 2.0 kcal/mol higher than by the BP86 method. Nevertheless, **TS(2c/trans-3c)** is still favorable than **TS(2a/trans-3a)**.

(39) Our preliminary calculation suggested that cis–trans isomerization requires a higher barrier with P–CO<sub>2</sub> ligand than with P–SO<sub>3</sub>.

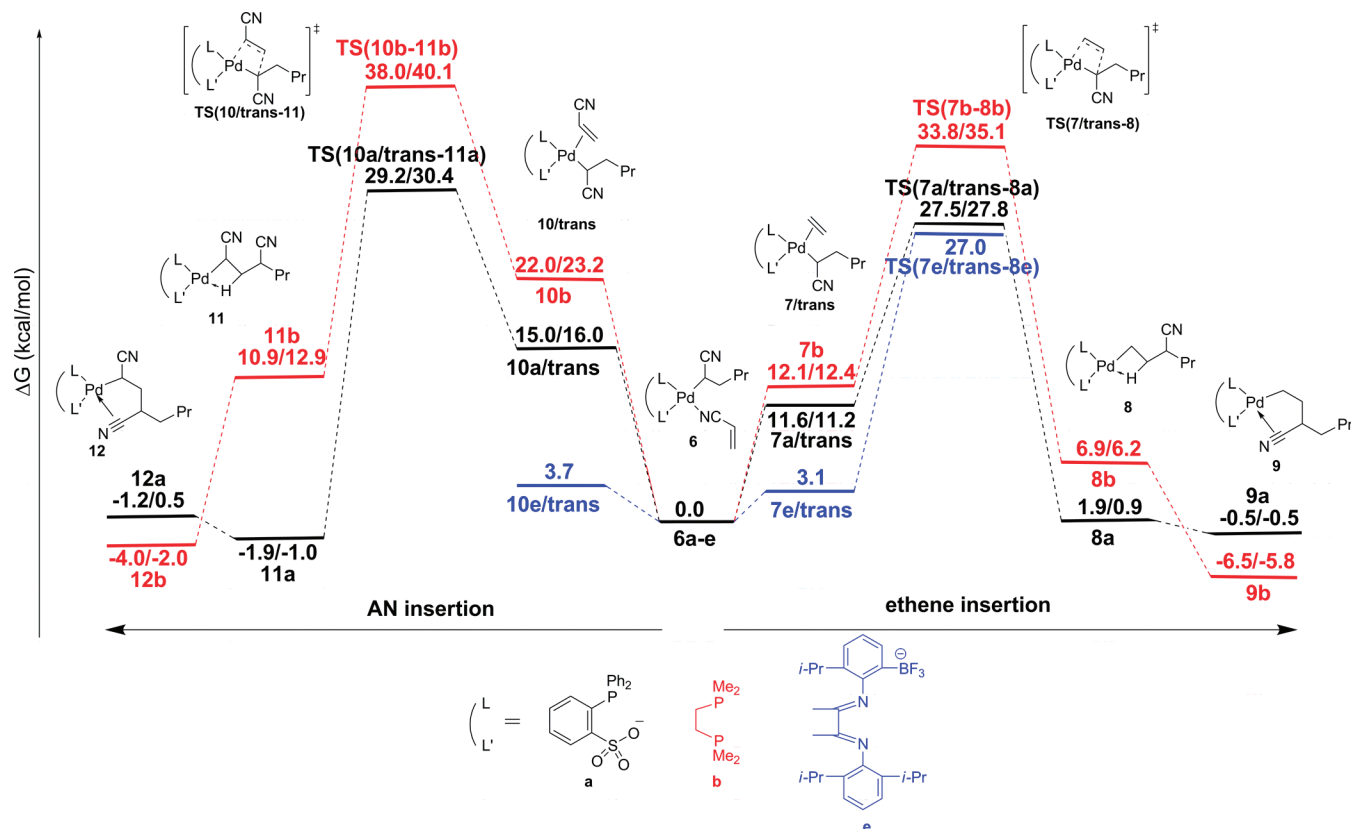


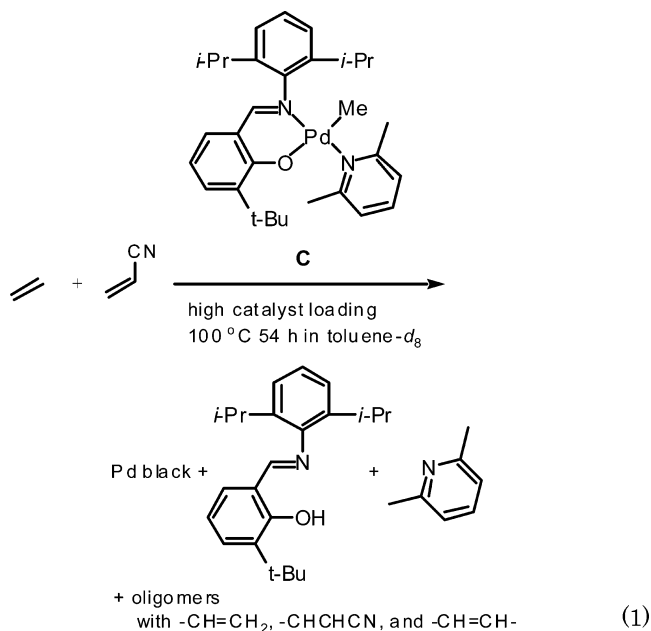
**Figure 3.** Energy profiles for the insertions starting from the  $\alpha$ -cyanoalkyl complexes **6a,b,e**. For complexes **6a** and **6b**, energies (E+ZPC, with zero-point energy correction, before /) and free energies (G, after /) are given in kcal/mol, relative to **6a** and **6b**, respectively. For complexes **6e**, the data were taken from ref 9 and free energy values (G) were expressed relative to **6e**.

**8a** isomerizes to the more stable product **9a** in which the nitrile group coordinates to the metal center by the  $\pi$ -electrons of the cyano group. In contrast to the possible ethylene insertion, successive AN insertion via **TS(10a/trans-11a)** is unlikely, since it requires a higher barrier of 29.2/30.4 kcal/mol relative to **6a**.

For the P–P system, TSs for both ethylene and AN insertions from **6b** are very high in energy, 33.8/35.1 and 38.0/40.1 kcal/mol relative to **6b**, respectively. The difference between the P–SO<sub>3</sub> complex and the P–P complex can be again attributed to the lower stability of the  $\pi$ -complexes **7** and **10** relative to the  $\sigma$ -AN complexes **6** for the cationic complex than the neutral complex; back-donation from the more electron-rich metal center to the  $\pi^*$ -orbital becomes more important and favorable in the neutral complexes. It is notable that the anionic diimine complex **6e** proposed by Piers and Ziegler<sup>9</sup> also showed higher stabilization of the  $\pi$ -complex **7e** or even more preferable ethylene insertion via **TS(7e/trans-8e)** than **TS(7a/trans-8a)** when compared to the P–SO<sub>3</sub> system.

**3. Attempted Ethylene/AN Copolymerization Catalyzed by the Neutral N–O/Pd Complex C.** The above-mentioned theoretical studies apparently imply that ethylene/AN copolymerization might be possible using anionic nitrogen-based ligands. Experimentally, however, no polymeric materials were given by using a N–O complex **C** as described in section 1 of this manuscript. In order to investigate the catalytic performance of complex **C** in detail, we exposed complex **C** to a mixture of ethylene/AN with high catalyst loading. When 0.25 mmol of complex **C** was treated with 0.3 mL of acrylonitrile in 3.0 mL of toluene-*d*<sub>8</sub> under ethylene (3.0 MPa) at 100 °C for 54 h, the peak for methylPd disappeared and the new peaks were

assignable to free N–OH, free lutidine and ethylene oligomers with both –CH=CH<sub>2</sub> and –CH=CHCN chain ends (Figure 4, eq 1).



As the rapid  $\beta$ -hydride elimination from alkylPd species was suggested by the chain ends of the oligomers, we further investigated the polymerization of ethylene in the absence of AN. After treatment of 0.01 mmol of **C** in 2.5 mL of toluene

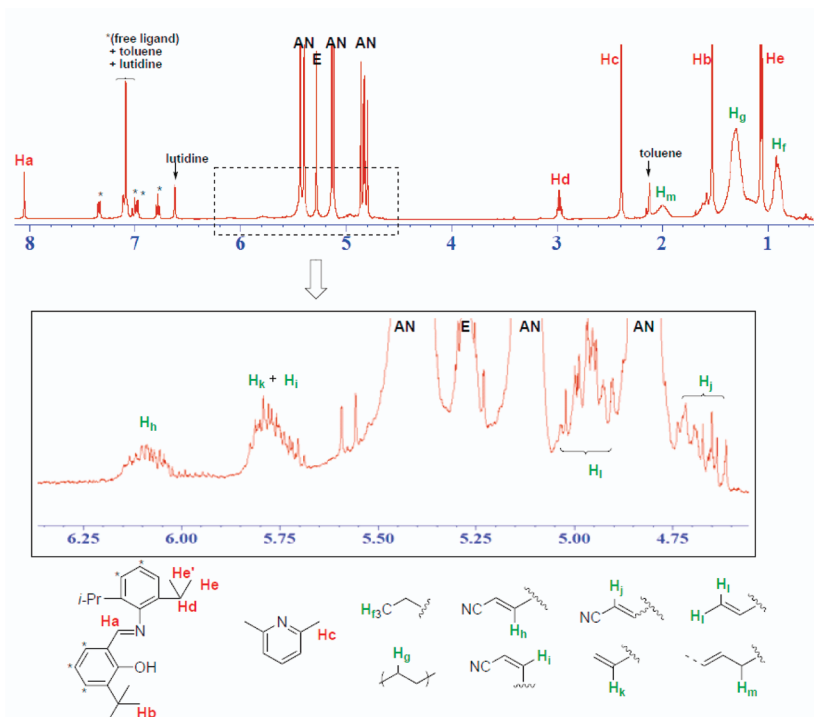


**Figure 4.**  $^1\text{H}$  NMR spectrum of the reaction of ethylene/AN with N–O/Pd complex **C** with high catalyst loading at 100 °C in toluene- $d_8$ . The peaks marked with an asterisk (\*) are due to free N–OH and the other peaks are assigned as ethylene (E), AN, and the protons labeled as Ha–Hm. Peaks other than ethylene and AN are assignable to free N–OH, free lutidine, and ethylene oligomer with both  $-\text{CH}=\text{CH}_2$  and  $-\text{CH}=\text{CHCN}$  chain ends.

under ethylene (3.0 MPa) at 100 °C for 5 days, only a trace amount of ethylene oligomer was afforded. The repeating unit was estimated to be ca. 10 on average, and the molar ratio of terminal alkene/internal alkene was 2.0/1.0. This is in sharp contrast to formation of 2.67 g of linear polyethylene using P– $\text{SO}_3$  complex **A** as a catalyst under the same condition in 15 h.<sup>21</sup> Reaction of ethylene with complex **C** was also monitored by  $^1\text{H}$  NMR spectra (see Supporting Information). We observed the disappearance of complex **C** and appearance of free N–OH and free lutidine. Simultaneously, a peak assignable to internal alkenes appeared.

Reaction of complex **C** with AN in the absence of ethylene also resulted in the insertion of AN followed by  $\beta$ -hydride elimination and release of free N–OH and free lutidine, that is, treatment of complex **C** with an excess amount of AN in toluene- $d_8$  at 100 °C for 54 h resulted in the formation of free N–OH, free lutidine, and an *E/Z* mixture of  $\text{CH}_3\text{CH}=\text{CHCN}$ .

Thus, most likely, the  $\beta$ -hydride elimination from alkylPd species took place to give [(N–O)PdH(alkene)] (**14f/trans**) and the resulting **14f/trans** underwent O–H reductive elimination (Scheme 6).<sup>40–42</sup> Consequently, unstable Pd(0) species and a free N–OH were provided. As is often the case, Pd(0) metal aggregates to form Pd black particles which catalyze isomerization of terminal alkenes into internal alkenes. In fact, precipitation of Pd black was found in the above experiments.

Accordingly, we next compared the P– $\text{SO}_3$  and N–O ligands in a viewpoint to see whether ethylene insertion is faster than  $\beta$ -hydride elimination from alkylPd species.

**4. Theoretical Studies on the  $\beta$ -Hydride Elimination from Alkyl–Pd Species and Subsequent Catalyst Decomposition to Release the Free Ligands.** In our previous study,<sup>32</sup> we proposed that the  $\beta$ -hydride elimination, which might cause branch-structure formation or chain-transfer reaction, is reasonably suppressed under the ethylene pressure in the ethylene polymerization reaction catalyzed by P– $\text{SO}_3$  complex **A**. The key species for this process is referred to Scheme 6, and the energy profile is summarized in Figure 5. There are two possible routes for  $\beta$ -hydride elimination, namely, **1a**  $\rightarrow$  **13a/cis**  $\rightarrow$  **TS(13a/cis-14a/trans)**  $\rightarrow$  **14a/trans** and **1a**  $\rightarrow$  **13a/cis**  $\rightarrow$  **TS13a(cis-trans)**  $\rightarrow$  **13a/trans**  $\rightarrow$  **TS(13a/trans-14a/cis)**  $\rightarrow$  **14a/cis**. As shown in Figure 5, relative to **1a**, the former route requires 29.9/20.2 kcal/mol and the latter needs 35.6/24.7 kcal/mol.

Here in this study, we calculated the  $\beta$ -hydride elimination process for the N–O complexes, starting from the  $\sigma$ -AN complex **1f** which corresponds to complex **C** in the real system. The results are shown in Scheme 6 and Figure 5. Notably, the  $\beta$ -hydride elimination product hydridopalladium species **14f/trans** with N–O ligand is quite stable at a much lower energy of 19.6/10.1 kcal/mol, compared to the corresponding species **14a/trans** with the P– $\text{SO}_3$  ligand of 29.1/19.5 kcal/mol. As a result, the barrier for  $\beta$ -hydride elimination via **TS(13f/cis-14f/trans)** to give **14f/trans** is also low (23.2/13.2 kcal/mol) in the N–O system, which is much lower than the corresponding TS for the P– $\text{SO}_3$  system (29.9/20.2 kcal/mol). Most likely, the weaker trans influence of the nitrogen ligand in the N–O system than the phosphine ligand in the P– $\text{SO}_3$  system causes a higher stability of the (N–O)PdH intermediate **14f/trans** and thus causes a lower reaction barrier for the  $\beta$ -hydride elimination.

As discussed in section 3, we observed catalyst decomposition to form palladium particles and free ligand in the reaction of complex **C** with ethylene or acrylonitrile. Accordingly, we calculated the energy levels for a sum of the free ligand and a

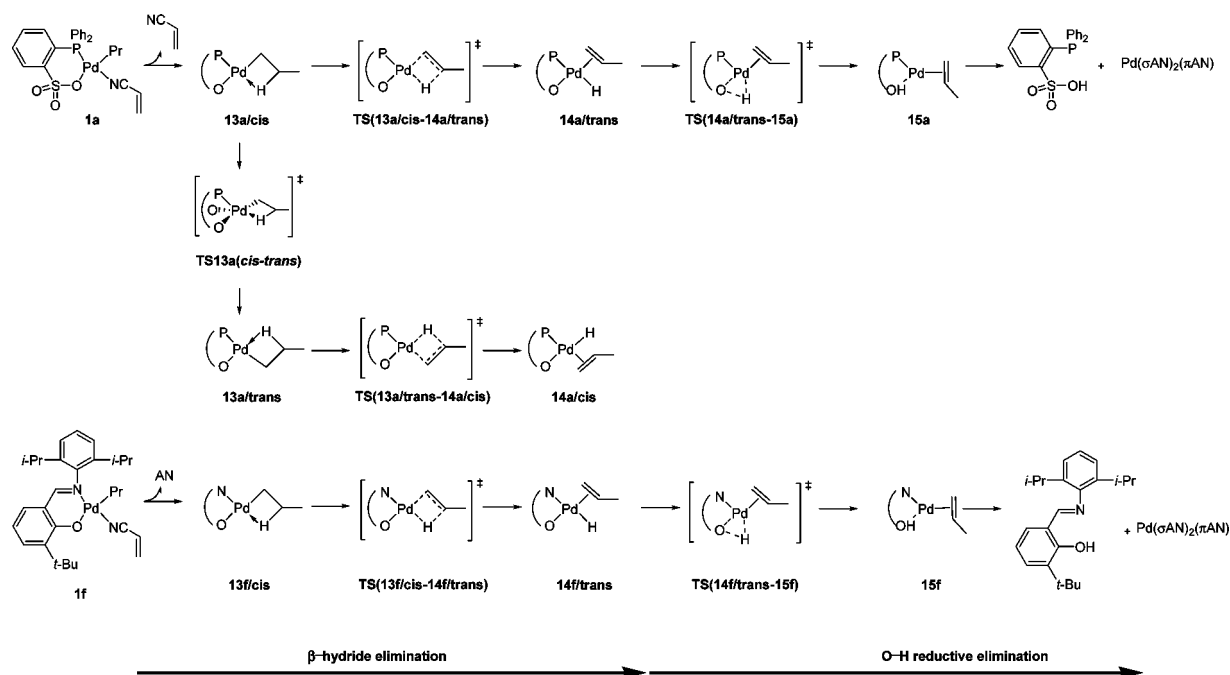
(40) Bugno, C. D.; Pasquali, M.; Leoni, P.; Sabatino, P.; Braga, D. *Inorg. Chem.* **1989**, 28, 1390–1394.

(41) Perez, P. J.; Calabrese, J. C.; Bunel, E. E. *Organometallics* **2001**, 20, 337–345.

(42) Amatore, C.; Jutand, A.; Meyer, G.; Carelli, I.; Chiarott, I. *Eur. J. Inorg. Chem.* **2000**, 1855–1859.



Scheme 6



zerovalent palladium, Pd( $\sigma$ -AN)<sub>2</sub>( $\pi$ -AN). For ligands Ph<sub>2</sub>P-SO<sub>3</sub>H (corresponding to **a**) and ArN-OH (corresponding to **f**), they were calculated to be 15.0/12.1 kcal/mol relative to **1a** and 9.1/5.5 kcal/mol relative to **1f**, respectively. Thus, release of the free ligand is thermodynamically favored for ArN-OH relative to **1f** than for Ph<sub>2</sub>P-SO<sub>3</sub>H relative to **1a** by 5.9/6.6 kcal/mol. On the other hand, we were unable to find a TS with lower energy for the reductive elimination from **14/trans** to **15** for

either P-SO<sub>3</sub> or N-O system. For example, a simple O-H reductive elimination processes both **14a/trans** → **TS(14a/trans-15a)** → **15a** and **14f/trans** → **TS(14f/trans-15f)** → **15f** required very high energy (46.1/35.1 kcal/mol for **TS(14a/trans-15a)** and 41.1/29.8 kcal/mol for **TS(14f/trans-15f)**); the values are much higher than the energy for ethylene insertion (20.3/21.8 kcal/mol for **TS(4a/trans-5a)** or 24.7 kcal/mol for **TS(4c/trans-5c)**).

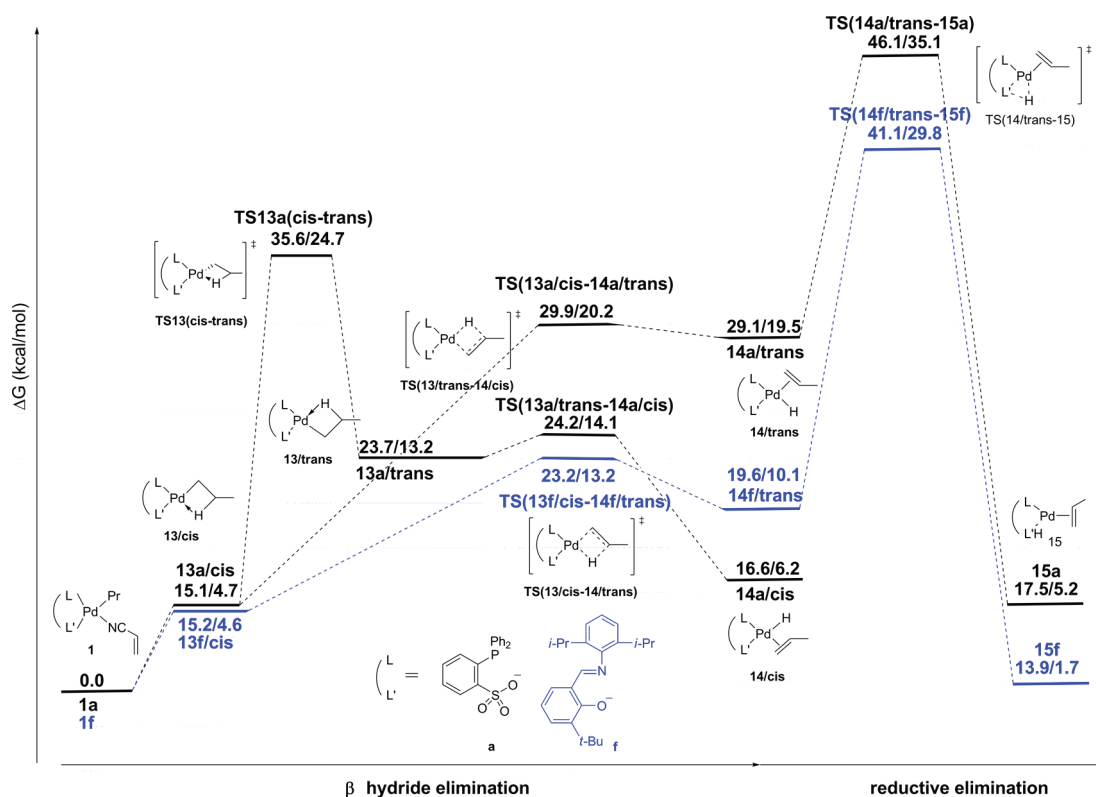
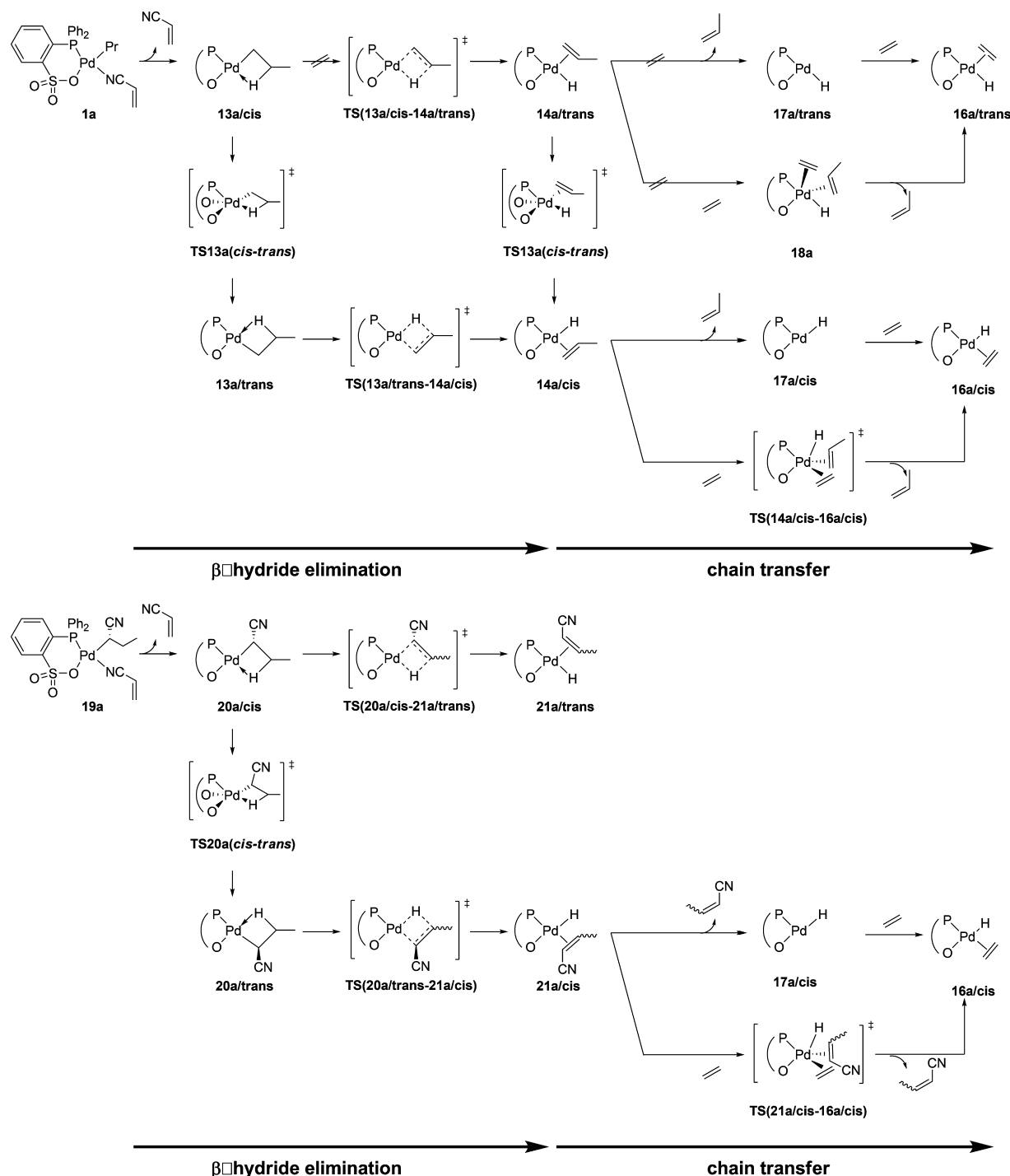


**Figure 5.** Energy profile (kcal/mol) for  $\beta$ -hydride elimination, and subsequent reductive elimination energies (E+ZPC, with zero-point energy correction, before / and free energies (G, after /) are given in kcal/mol, relative to **1a** and **1f**.

Scheme 7



**5. Theoretical Studies on the Chain-Transfer Reaction.** In this section, we studied the chain-transfer reaction subsequent to  $\beta$ -hydride elimination, which determines the molecular weight and chain-end structure of the copolymer. The key intermediates and transition states are shown in Scheme 7. In addition, calculation results are roughly sketched in Figures 6 and 7.

As we reported previously,<sup>32</sup> the chain-transfer reaction from the trans isomer of the hydridoPd complex **14a/trans** requires quite high energy both in a dissociative (61.1/38.2 kcal/mol for **18a**) and associative manner (30.7/32.5 kcal/mol for **17a/trans**). The most probable fate of **14a/trans** is reinsertion of propylene to form **13a/cis**. The lowest energy route for the chain-transfer reaction following  $\beta$ -hydride elimination is through the cis

isomer of the hydridoPd complex **14a/cis**, namely, **1a**  $\rightarrow$  **13a/cis**  $\rightarrow$  **TS13a(cis-trans)**  $\rightarrow$  **13a/trans**  $\rightarrow$  **TS(13a/trans-14a/cis)**  $\rightarrow$  **TS(14a/cis-16a/cis)**  $\rightarrow$  **16a/cis**, with an activation energy of 35.6/24.7 kcal/mol relative to **1a**.

We further calculated the corresponding chain-transfer pathway starting from  $\alpha$ -cyanoalkylPd complex, **19a**  $\rightarrow$  **20a/cis**  $\rightarrow$  **TS20a(cis-trans)**  $\rightarrow$  **20a/trans**  $\rightarrow$  **TS(20a/trans-21a/cis)**  $\rightarrow$  **TS(21a/cis-16a/cis)**  $\rightarrow$  **16a/cis**. The energy profile of this reaction is not quite different from that starting from **1a** but with a little higher energy for all the intermediates and transition states. The highest energy barrier in the process is 40.6/28.0 kcal/mol via **TS20a(cis-trans)** relative to **19a**.

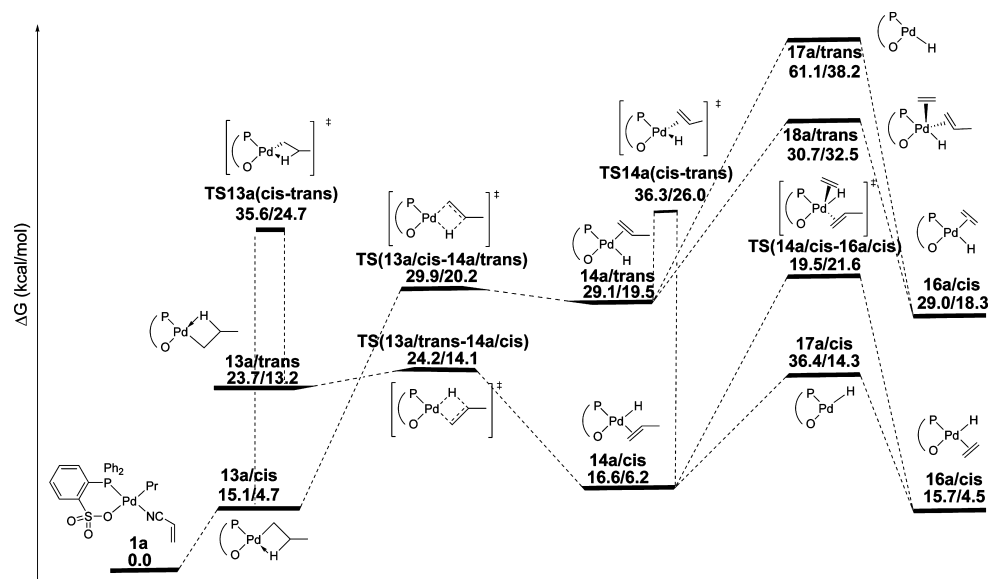


**Figure 6.** Energy profile (kcal/mol) for  $\beta$ -hydride elimination and subsequent chain-transfer reaction from alkylPd(P-SO<sub>3</sub>). Energies (E+ZPC, with zero-point energy correction, before /) and free energies (G, after /) are given in kcal/mol, relative to **1a**.

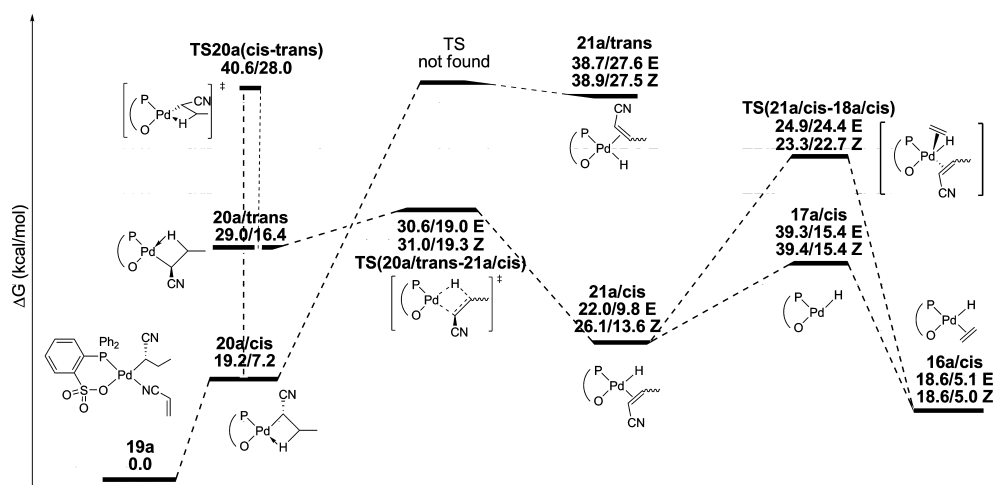


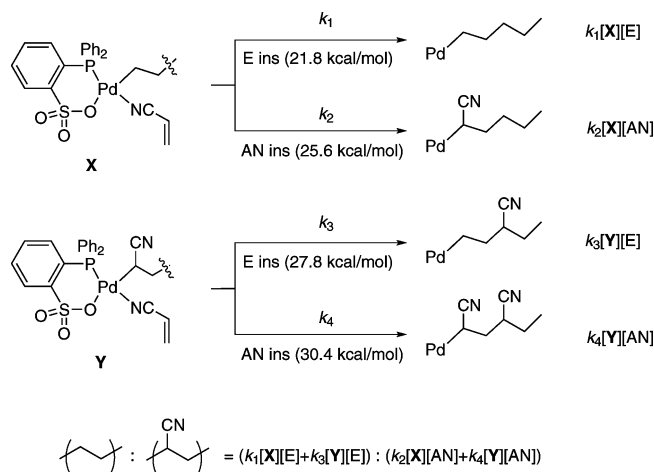
**Figure 7.** Energy profile (kcal/mol) for  $\beta$ -hydride elimination and subsequent chain-transfer reaction from  $\alpha$ -cyanoalkylPd(P-SO<sub>3</sub>). Energies (E+ZPC, with zero-point energy correction, before /) and free energies (G, after /) are given in kcal/mol, relative to **20a**.

**6. Theoretical Elucidation on the Experimentally Obtained Data: The Ethylene/AN Incorporation Ratio and Chain End Structure of the E/AN Copolymer.** Now, on the basis of all these calculations described above, we can estimate the E/AN unit ratios in the chains and at the terminating chain ends. Both values nicely matched to the experimental data we reported previously.<sup>21</sup>

#### 6.1. Ethylene/AN Incorporation Ratio of the E/AN Copolymer.

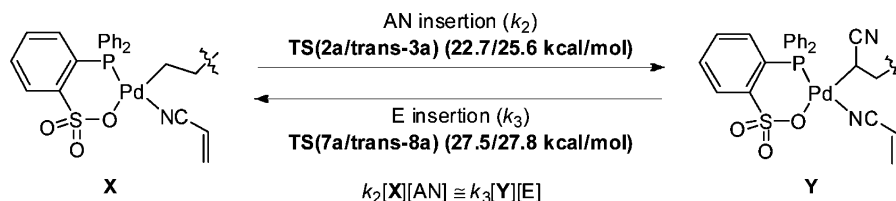
The incorporation ratio of ethylene and AN can be estimated from (1) the rate constants of ethylene or AN insertion to **X** and **Y**, (2) the ethylene and AN concentrations, [E] and [AN], in the reaction mixture, and (3) the concentrations of alkylPd complex **X** and  $\alpha$ -cyanoalkylPd complex **Y**, according to the equation shown in Scheme 8. While the rate constants for the insertion steps,  $k_{1-4}$ , can be derived from the theoretically calculated  $\Delta G$  values, [E]:[AN] was obtained experimentally by high-pressure NMR spectroscopy.<sup>43</sup> When a mixture 0.5 mL of acrylonitrile and 4.5 mL of toluene-*d*<sub>6</sub> was pressurized to 1.0 MPa with ethylene at 50 °C, the observed [E]:[AN] was 1:20. On the basis of this value, the [E]:[AN] ratio was extrapolated to be 1:10 under the reaction conditions, 3.0 MPa

#### Scheme 8

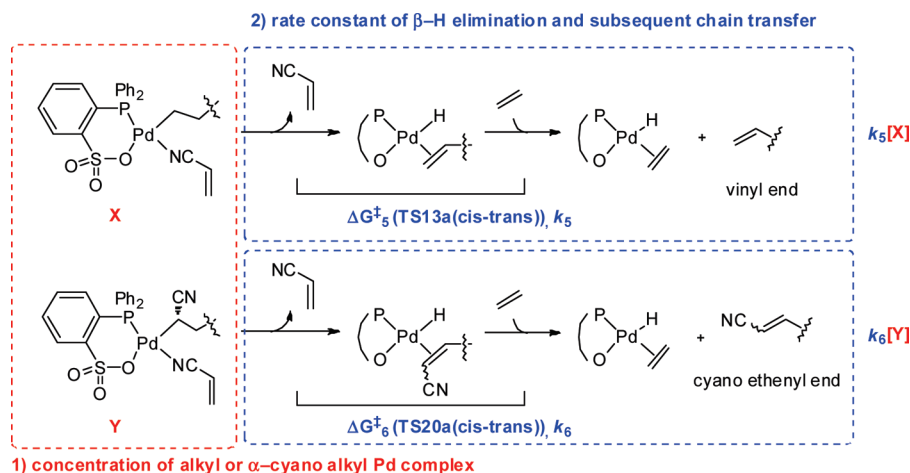


of ethylene at 100 °C.<sup>44</sup> Because the concentrations of **X** and **Y** during copolymerization were difficult to measure directly, we applied the steady-state approximation of these concentra-

Scheme 9. Steady State Approximation of X and Y



Scheme 10



tions as described in Scheme 9. Assuming that most of the Pd complexes present in the reaction mixture are either **X** or **Y**, conversion of **X** to **Y**, AN insertion to **X**, should proceed at about the same rate as that of **Y** to **X**, E insertion to **Y**. As discussed in sections 2 and 3, the barrier for AN insertion to alkylPd complex is 22.7/25.6 kcal/mol and that for E insertion to  $\alpha$ -cyanoalkylPd complex is 27.5/27.8 kcal/mol; therefore,  $k_2$ : $k_3$  is estimated to be about 1:18 at 373.15 K. Therefore, the concentration ratio of alkylPd complex **X** and  $\alpha$ -cyanoalkylPd complex **Y** is expected to be 1:180 under the conditions where  $[\text{E}]:[\text{AN}]$  is 1:10. On the basis of the obtained concentration ratios and the rate constants, the AN incorporation ratio can be estimated as 8 mol % when copolymerization is carried out in 9:1 toluene/AN with 3.0 MPa of ethylene. This estimation is in good agreement with the experimental value for AN incorporation (3.2%) obtained under the reaction conditions.<sup>21,45,46</sup>

**6.2. Chain End Structure of the E/AN Copolymer.** Experimentally, two terminating chain end structures were detected for the E/AN copolymer. Vinyl ( $-\text{CH}=\text{CH}_2$ ) group was found at 20% of the chain ends and the rest was the  $\beta$ -cyanoethenyl ( $-\text{CH}=\text{CHCN}$ ) group under the polymerization conditions: acrylonitrile, 2.5 mL; toluene, 2.5 mL; ethylene, 3.0 MPa at 100 °C. The ratio of the vinyl and  $\beta$ -cyanoethenyl chain ends

can also be estimated from (1) the concentration of alkylPd complex **X** and  $\alpha$ -cyanoalkylPd complex **Y** and (2) the rate constants of the  $\beta$ -hydride elimination and subsequent chain-transfer reaction (Scheme 10). As shown in Figures 6 and 7, the calculated energy barriers for the chain-transfer reaction from the alkylPd complex and the  $\alpha$ -cyanoalkylPd complex are 35.6/24.7 kcal/mol and 40.6/28.0 kcal/mol, respectively, and based on these values, the ratio of  $k_5$ : $k_6$  is calculated to be 78:1. Considering that the  $[\text{X}]/[\text{Y}]$  ratio is 1/900 under the experimental conditions, the ratio of the vinyl and cyanoethenyl chain ends is now estimated to be 8:92. The value is quite reasonable compared to the experimental result of 20:80.<sup>47</sup>

## Conclusion

Throughout the studies, two characteristic features of the P-SO<sub>3</sub> ligand have been revealed: (1) The P-SO<sub>3</sub> ligand facilitates both AN insertion to alkylPd and ethylene insertion to  $\alpha$ -cyanoalkylPd when compared to P-P ligand. The difference can be attributed to destabilization of the  $\sigma$ -AN complex **1** relative to the  $\pi$ -AN complex **2** by the anionic ligand. This seems to be characteristic for any kinds of anionic ligands, namely, for both P-SO<sub>3</sub> and N-O. (2) The  $\beta$ -hydride elimination is reasonably suppressed with P-SO<sub>3</sub>. As suggested in our previous study,<sup>32</sup>  $\beta$ -hydride elimination from alkylPd **1a**, that is **TS(13a/cis-14a/trans)**, requires a rather higher barrier with P-SO<sub>3</sub>. Even more importantly, here we found that the chain transfer proceeds not from **14a/trans** but from **14a/cis**. As a result, the most probable chain-transfer route is **1a**  $\rightarrow$  **TS13a(cis-trans)**  $\rightarrow$  **13a/trans**  $\rightarrow$  **TS(13a/trans-14a/cis)**  $\rightarrow$  **14a/cis**  $\rightarrow$  **TS(14a/cis-16a/cis)**  $\rightarrow$  **16a/cis**. The highest barrier for this chain transfer is the cis/trans isomerization **TS13a(cis-trans)** of 24.7 kcal/mol, which is even higher than

(43) See Supporting Information for details of the discussion.

(44) Lee, L. S.; Ou, H. J.; Hsu, H. L. *Fluid Phase Equilib.* **2005**, *231*, 221–230.

(45) All the thermochemical calculations in this paper are done at 298.15 K. The key intermediates and transition states **1a**, **TS(2a/trans-3a)**, **1c**, and **TS(2c/trans-3c)** were calculated at 373.15 K (polymerization condition). **TS(2a/trans-3a)** is 22.7/26.6 kcal/mol relative to **1a**. **TS(2c/trans-3c)** is 21.8/25.6 kcal/mol relative to **1c**. Therefore, there is little effect of ligands on the temperature dependency on the free energy.

(46) Because the ratio of experimental value/calcd value can be drawn as  $\exp((\Delta G(\text{exp}) - \Delta G(\text{calcd}))/RT)$ , the difference in  $\Delta G$ , that is  $\Delta(\Delta G) = \Delta G(\text{exp}) - \Delta G(\text{calcd})$  can be calculated as  $\Delta(\Delta G) = RT \ln(\text{exp/calcd}) = 8.314 \cdot 373.15 \cdot \ln((8/92)/(3.2/96.8))/(4.1 \cdot 1000) = 0.732$ .

(47)  $\Delta(\Delta G) = \Delta G(\text{exp}) - \Delta G(\text{calcd}) = 8.314 \cdot 373.15 \cdot \ln((8/92)/(20/80))/(4.1 \cdot 1000) = -0.799$ .

**TS(13a/cis-14a/trans)** of 20.2 kcal/mol.  $\beta$ -Hydride elimination from  $\alpha$ -cyanoalkylPd **15a** (relevant to **6a**) and its subsequent chain transfer also requires a high energy at **TS(20acis-trans)** of 28.0 kcal/mol. In sharp contrast to the copolymer production by catalyst **A** with P-SO<sub>3</sub>, complex **C** with N-O ligand resulted in rapid  $\beta$ -hydride elimination from both alkylPd species and  $\alpha$ -cyanoalkylPd in our experiments. The resulting (N-O)PdH seems to release free N-OH and Pd black particles that terminated polymerization to finally end up in catalyst decomposition. The  $\beta$ -hydride elimination, chain-transfer, and catalyst decomposition processes were also theoretically studied. Finally, using the values we calculated, we could estimate the E/AN incorporation ratio and chain end structure of the E/AN copolymer obtained by catalyst **A**. Both values nicely matched the experimental data we previously reported. Thus, we believe the overall experimental and theoretical results should help in designing new ligands for challenging copolymerizations.

**Acknowledgment.** The authors are grateful to Prof. Jerome Claverie (University of Quebec, Montreal) and Mr. Akifumi Nakamura (The University of Tokyo) for helpful discussions. Computer resources for theoretical calculations were mainly provided by the Research Center for Computational Science in the National Institutes of Natural Sciences. L.W.C. acknowledges the Fukui Institute Fellowship. This work was in part supported by the Grant-in-Aid for Scientific Research No. 21245023 from JSPS and by the Japan Science and Technology Agency (JST) with a Core Research for Evolutional Science and Technology (CREST) grant in the Area of High Performance Computing for Multiscale and Multiphysics Phenomena.

**Supporting Information Available:** Complete ref 36 experimental detail, addition data, structures, and calculation results. This material is available free of charge via the Internet at <http://pubs.acs.org>.

JA104837H